

DENSE CORES IN DARK CLOUDS. VII. LINE WIDTH–SIZE RELATIONS

G. A. FULLER^{1,2} AND P. C. MYERS¹*Received 1991 May 7; accepted 1991 July 15*

ABSTRACT

Observations of 14 dense cores in lines of CS, C¹⁸O and NH₃ are combined to examine the relations between the Doppler width of a line and the spatial extent of the map of line intensity. The line width increases with map size R as R^p . The deduced width Δv_{TOT} of the velocity distribution of the molecule of mean mass has $p = 0.20 \pm 0.04$, and the deduced width Δv_{NT} of the nonthermal velocity distribution has $p = 0.7 \pm 0.1$. The values of p for eight cores with embedded stars and for six cores without embedded stars are statistically indistinguishable, but p is better determined for cores without stars. Thus the physical basis of the line width–size relations is part of the initial conditions for star formation, rather than a consequence of the star-core interaction. The cores appear close to virial equilibrium, consequently the variation of number density with distance r from the core density maximum is deduced. Expressed as a single power law, the number density varies as r^{-q} , with $q = 1.6 \pm 0.1$, and the nonthermal pressure varies as r^{-s} , with $s = 0.2 \pm 0.1$. If the nonthermal pressure is magnetic, the field strength increases with density as $B \propto n^{0.05}$. The density variation within the cores is also deduced for a model where the thermal and nonthermal motions imply two corresponding power law components of density.

Subject headings: ISM: kinematics and dynamics — ISM: molecules — radio lines: molecular: interstellar

1. INTRODUCTION

Many observations of molecular lines in interstellar clouds have revealed two types of relation of the form $\Delta v_{\text{obs}} \sim R^p$ between Δv_{obs} , the characteristic FWHM velocity width of a line observed in a particular cloud, and R , the characteristic size of the cloud map of the intensity of the same line. Observations of tens to hundreds of clouds in the same line indicate a “cloud-to-cloud” correlation with p close to 0.5, in the 2.6 mm line of ¹²CO (Dame et al. 1986; Scoville, Sanders, & Clemens 1986; Solomon et al. 1987), in the 2.7 mm line of ¹³CO (Leung, Kutner, & Mead 1982), and in the 13 mm line of NH₃ (Torrelles et al. 1983). Observations of one or a few clouds in several lines indicate a line-to-line correlation with p in the range 0.25 to 0.75 (Martin & Barrett 1978; Myers et al. 1978; Snell 1981). Larson (1981) summarized other observations showing similar line to line correlations within clouds.

Several authors have combined these two types of correlation, by considering Δv_{obs} versus R for many tens of clouds, in more than one line (Larson 1981; Myers 1983; Falgarone & Perault 1987; Myers & Goodman 1988). The combination increases the range of Δv_{obs} and R , yielding correlations of increased significance, with p again near 0.5.

When $p = 0.5$, and when the observed lines are primarily nonthermal, the cloud-to-cloud relations are consistent with virial equilibrium, combined with a relative variation from cloud to cloud in the column density or the internal pressure, which is smaller than the relative variation from cloud to cloud in the cloud size. This small variation could arise for several possible reasons, including a combination of sensitivity and selection (Larson 1981; Kegel 1989); cloud stability (Chieze 1987); equipartition between magnetic and kinetic energy (Myers & Goodman 1988); external pressure (Fleck 1988;

Elmegreen 1989); or the effects of star formation (McKee 1989). The cloud-to-cloud relations have also been interpreted as indicating a turbulent cascade of energy from large to small scales (Larson 1981; Fleck 1983; Myers 1983).

The line-to-line relations in a cloud pertain to the spatial structure of the cloud motions and density structure of the cloud. They are less likely to arise from a narrow range of column density than are the cloud-to-cloud relations, since p departs more from 0.5 and since the use of several lines increases the range of column density to which the observations are sensitive. These relations have received relatively little attention.

In this paper we report on correlations between the line width and size for observations of three lines in each of 14 dark cloud cores. The data are based on the 13 mm NH₃ line data of Benson & Myers (1989, hereafter BM) and on data from the 3.0 mm CS line and the 2.7 mm C¹⁸O line observed by Fuller (1989). We report both the core-to-core and line-to-line variation within cores. The CS and C¹⁸O lines sample the more extended core gas, whose motion is predominantly nonthermal whereas the NH₃ line samples the less extended, primarily thermal gas. Therefore, these data can distinguish between the nonthermal and the total line width (Myers 1983) and the variation of each with core size.

2. OBSERVATIONS

In the analysis presented here the sizes and line widths are obtained from the observed data in the manner described in Myers et al. (1991a). The ammonia size is the geometric mean of the half-peak radii determined from two-dimensional Gaussian fits to the ammonia peak temperature map quoted in BM. These radii, typically 0.05 pc, have been corrected for the smoothing of the telescope beam. For the one core in this sample not mapped by BM, L1535, the NH₃ observations of Ungerechts, Walmsley, & Winnewisser (1982) have been used. The data at larger size scales are from the CS $J = 2 \rightarrow 1$ and

¹ Postal address: Harvard-Smithsonian Center for Astrophysics, Mail Stop 42, 60 Garden Street, Cambridge, MA 02138.

² Also with Astronomy Department and Radio Astronomy Laboratory, University of California, Berkeley.

TABLE 1
OBSERVED LINE WIDTHS AND SIZES

CORE	C ¹⁸ O		CS		NH ₃	
	Δv_{OBS} (km s ⁻¹)	R (pc)	Δv_{OBS} (km s ⁻¹)	R (pc)	Δv_{OBS} (km s ⁻¹)	R (pc)
Cores with Stars						
B35	0.88	0.21	1.10	0.24	0.82	0.21
B5	0.86	0.36	0.92	0.26	0.34	0.23
L1152	0.57	0.32	0.53	0.18	0.33	0.11
L1262A	0.74	0.12	0.69	0.12	0.37	0.06
L1489	0.49	0.08	0.65	0.07	0.28	0.03
L1535	0.48	0.14	0.62	0.10	0.30	0.05
L255	0.53	0.17	0.45	0.15	0.21	0.04
L43B	0.52	0.13	0.64	0.14	0.40	0.07
Starless Cores						
L134A	0.51	0.28	0.62	0.12	0.32	0.07
L1400G	0.52	0.16	0.66	0.11	0.30	0.07
L1498	0.43	0.19	0.32	0.06	0.20	0.03
L1512	0.31	0.14	0.30	0.09	0.21	0.02
L234A	0.44	0.16	0.54	0.17	0.23	0.05
L63	0.35	0.13	0.54	0.18	0.26	0.06

C¹⁸O $J = 1 \rightarrow 0$ observations of Fuller (1989). The sizes and line widths are tabulated in Table 1. The CS and C¹⁸O observations were made with the NRAO 12 m telescope³ between 1986 and 1987 and the FCRAO 14 m telescope⁴ between 1985 and 1988, respectively. The size of the CS and C¹⁸O maps is defined as the radius of the circle with area equal to the area of the half peak contour of the line peak temperature maps. No correction has been applied for the smoothing effect of the beam as the measured map radii are 3–16 times the radius of the beam used for the observations. We estimate the statistical uncertainties in the size to be between 0.01 and 0.03 pc.

The CS and C¹⁸O line widths quoted are the median line widths over the maps. The velocity resolution of most of the observations were 0.31 and 0.27 km s⁻¹ for the CS and C¹⁸O, respectively. A few maps were made with either 0.09 or 0.07 km s⁻¹ resolution for the CS and C¹⁸O, respectively. The line widths have been corrected for the spectrometer response. The ammonia line width is taken from the multicomponent analysis presented in BM and is the FWHM of a single hyperfine NH₃ component, corrected for broadening by optical depth and spectrometer resolution. The estimated uncertainties in the line widths are between 0.1 and 0.05 km s⁻¹.

The sample of cores in this work comprises two subsamples: eight cores which have an *IRAS* source within one ammonia map half-peak diameter of the ammonia peak and six cores with no *IRAS* sources within this distance of the core peak. For the cores at a distance of 140 pc, which is typical of the sample, and the reddest spectrum consistent with the observations of *IRAS* sources embedded in nearby cores (Myers et al. 1987), the *IRAS* point source upper limits constrain the luminosity of any undetected sources to be $< 0.1 L_{\odot}$. The typical luminosity of the eight associated stars is $2 L_{\odot}$.

³ Operated by Associated Universities, Inc., under cooperative agreement with the National Science Foundation.

⁴ The Five College Radio Astronomy Observatory is supported by the Commonwealth of Massachusetts and the National Science Foundation and is operated with the permission of the Metropolitan Commission.

3. RESULTS

3.1. The Observed Line Width

The line width versus radius of the emission region for eight dense cores associated with young stars and six starless dense cores are shown in Figures 1a and 1b, respectively. It is clear that both cores with stars and those without stars show a statistically significant increase of the line width with the extent of the molecular emission. A linear fit to the data in Figures 1a and 1b gives for the starless cores,

$$\log(\Delta v_{\text{obs}}) = (0.44 \pm 0.08) \log(R) + (0.01 \pm 0.08),$$

$$\text{CC} = 0.74 \quad (1)$$

and for the cores with stars

$$\log(\Delta v_{\text{obs}}) = (0.4 \pm 0.1) \log(R) + (0.14 \pm 0.09),$$

$$\text{CC} = 0.65 \quad (2)$$

where Δv_{obs} is the observed line full width at half-maximum, R is the core radius and CC is the Spearman rank correlation coefficient. The uncertainties are one standard deviation, based on the scatter about the best fit. The slopes of these correlations are consistent with the values derived from ¹³CO and NH₃ by Myers (1983).

There is significantly less scatter in the correlation for the cores without stars: the standard deviation of the residuals from the fit given above is 0.09 for the starless cores and 0.13 for the cores with stars. Most of the scatter in the cores without stars arises from the CS points. If the CS data are excluded, the slope decreases slightly to 0.39 ± 0.05 and the standard deviation on the residuals drops significantly to 0.05. However, excluding the CS data for the cores with stars changes neither the slope of the correlation nor the standard deviation of the residuals. Thus the larger scatter in the cores with stars is probably not dominated by a single molecule, as it is for the cores without stars, but is rather a property of the ensemble of the observations.

The line width also increases with map size from line to line within most cores. For the six cores without stars, the slope of the best-fit line to the three measurements for each core has mean \pm standard error of the mean of 0.47 ± 0.09 , consistent with slope of the best-fit line to all the data given in equation (1). This consistency indicates the correlation shown in Figure 1a and equation (1) is due largely to the variation of line width with size within the cores in the sample rather than to any core-to-core variation. This consistency is evident in Figure 1c, which identifies the observations of each starless core. However the cores with stars show no such consistency. The three-point fits for the eight cores with stars have slopes with mean \pm standard error of the mean of 0.95 ± 0.18 , significantly larger than the slope of 0.4 ± 0.1 for the correlation of all the data taken together. If the two cores with the most luminous stars, B35 and B5, are excluded the mean slope within a core containing a star decreases to 0.65 ± 0.06 , still somewhat steeper than the slope for all the data from cores with stars. If the same two cores are excluded from the fit to all the data for the cores with stars, the slope of the correlation and the standard deviation of the residuals remain essentially unchanged but the statistical significance of the correlation decreases.

3.2. The Total and the Nonthermal Line Width

As described above the cores without stars have less scatter in their line width–size relation and more consistency between

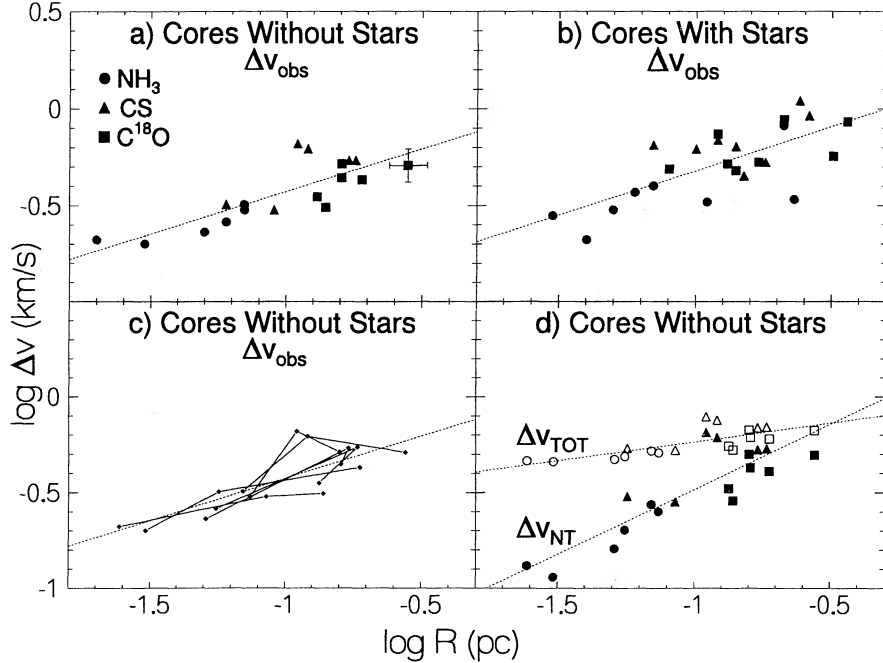


FIG. 1.—The line width–size correlations for the observed cores. The upper panels show the observed line FWHM, Δv_{obs} , vs. size of the emission region, R , for (a) the cores without embedded stars (L1498, L1400G, L1512, L134A, L234A, L63) and (b) cores associated with young stars with luminosities between 0.4 and $15 L_{\odot}$ (B5, L1489, L1535, B35, L43B, L255, L1152, L1262A). In each of these two panels the measurements from the C^{18}O , CS, and NH_3 are shown by different symbols. The broken line in each panel shows the best fit line to the data given in eqs. (1) and (2). The errors bars show the estimated typical uncertainty in the determined size and line width. (c) This panel shows again the data for the starless cores but with the three measurements for each core connected by line segments. The broken line indicates the best-fit line from eq. (1). (d) The variation of the nonthermal component of the observed line widths, Δv_{NT} (filled symbols), and the total velocity width, Δv_{TOT} (open symbols), with size for the starless cores are shown. The shapes of the symbols indicate the molecular tracer as in (a). The broken lines show the correlations given in eqs. (4) and (5).

their relations for all the data and for the line to line data. Therefore, we concentrate on the starless cores in the following discussion.

The observed molecules are only trace components of the dense gas, and it is the velocity dispersion, or equivalently, the velocity width, Δv_{TOT} , of the average molecule which is important for discussion of the gas kinetic energy. The motions of the molecule of mean mass m ($= 2.33$ amu) are assumed to consist of a component due to the thermal motions of the molecule plus a nonthermal component Δv_{NT} (Myers 1983; Myers, Ladd, & Fuller 1991b, hereafter MLF). Thus

$$\Delta v_{\text{TOT}}^2 = 8 \ln 2 \frac{kT}{m} + \Delta v_{\text{NT}}^2 = \Delta v_{\text{obs}}^2 + 8 \ln 2kT \left(\frac{1}{m} - \frac{1}{m_{\text{obs}}} \right), \quad (3)$$

where m_{obs} is the mass of the observed molecule, k is the Boltzmann constant, and T is the kinetic temperature which will be taken to be 10 K, consistent with those derived by BM. For the starless cores, it is found that

$$\log(\Delta v_{\text{TOT}}) = (0.20 \pm 0.04) \log(R) - (0.05 \pm 0.04), \quad (4)$$

and

$$\log(\Delta v_{\text{NT}}) = (0.7 \pm 0.1) \log(R) + (0.2 \pm 0.1). \quad (5)$$

These correlations are shown in Figures 1d. As with Δv_{obs} , the cores with stars show correlations of Δv_{TOT} and Δv_{NT} with R which are consistent with these correlations for the starless cores but which have more scatter.

4. DISCUSSION

4.1. Nonthermal Line Broadening

The increase in line width with map size is evidently a property of the *nonthermal* part of the line width, since Δv_{NT} dominates Δv_{TOT} for nearly all of the data in Figure 1, and since the slope of the line width–size relation for Δv_{NT} is 0.7, significantly steeper than the slope of Δv_{TOT} , 0.2. The line widths of both the C^{18}O and CS, even when corrected for the saturation broadening (see below), are in excess of the thermal width. Therefore the correlation length of the nonthermal motions in these C^{18}O and CS cores is probably significantly smaller than the spatial extent of these lines. The physical basis of the nonthermal line widths has been widely discussed (see, e.g., MLF and references therein). Spectral lines can be broadened beyond their thermal widths by effects of supersonic stellar winds, optical depth, and magnetic or nonmagnetic waves or “turbulence.” MLF suggest that the nonthermal part of the line width cannot arise primarily from stellar winds, based on data from cores with stars. The data presented here support this point, since the increase in Δv_{NT} with R is best defined for starless cores, where stellar winds can have no significant effects.

In this subsection we suggest that nonthermal line broadening by stellar winds and optical depth probably contribute to the scatter in the line width–size relations in the present sample, but do not substantially change their slopes.

The slope of the line width–size correlation does not depend on the presence of a star, but the cores containing stars have a larger scatter about the best-fit line than do the starless cores. The increased scatter might arise because cores which form

stars have a larger dispersion in properties and/or because of the effects of outflows and stellar winds. Six of the stars in the cores shown in Figure 1b are known to have CO outflows, and one other, L1152, has other evidence suggesting the presence of an outflow (Goldsmith, Langer, & Wilson 1986; Heyer et al. 1987; Myers et al. 1988; Parker et al. 1988). It is possible that these outflows are stirring the core material and hence increasing the dispersion about the underlying line width–size correlation.

There are several cores in which the CS line is broader than the $C^{18}O$ line, even though the CS traces a somewhat smaller region. A possible explanation of this, and the enhanced scatter of the CS measurements in the starless cores, is that high optical depth in the CS contributes to the observed line width and there is some variation in CS optical depth between different cores. For example, if the CS is intrinsically tracing material with a velocity dispersion 80% of the velocity dispersion of the material traced by the $C^{18}O$, then optical depth broadening of the CS could account for the $\sim 20\%$ enhancement of the CS line over that of the $C^{18}O$ if the CS optical depth is 3 or more (Phillips et al. 1979). The detection of $C^{34}S$ in several of these cores demonstrates that the CS is optically thick in these cores with peak optical depths of ~ 3 (Zhou et al. 1989; Fuller 1989).

4.2. The Density Structure within a Core

The correlations of Δv_{obs} with map size R (eqs. [1] and [2]) have slopes consistent with many previous determinations where Δv_{obs} is dominated by nonthermal motions (e.g., Leung et al. 1982; Scoville et al. 1986; Dame et al. 1986; Solomon et al. 1987), but this “agreement” can be misleading. For discussions of cloud kinetic energy and support the physically important quantity is Δv_{TOT} , not Δv_{obs} . When the line width is highly nonthermal as in giant molecular clouds (e.g., Dame et al. 1986; Scoville et al. 1986), Δv_{obs} , Δv_{NT} , and Δv_{TOT} are indistinguishable. The cores observed in this work have significantly less turbulence than do most molecular clouds, so that the observed line widths do not directly reflect the velocity dispersion for the molecule of mean mass. In these cores $\Delta v_{\text{TOT}} \propto R^{0.2}$ (eq. [4]) which is significantly flatter than the correlation for Δv_{obs} with size (eqs. [1] and [2]) and $\Delta v_{\text{TOT}}(R)$ derived from the observations of many other clouds (e.g., Dame et al. 1986; Snell 1981).

As described above, the mean slope of the line width with size within an individual starless core is consistent with the observed trend for the whole sample of starless cores. Thus the correlations given in equations (1), (4), and (5), reflect internal properties of the starless cores. Since the cores are close to virial equilibrium (Myers et al. 1991), the dependence of Δv_{TOT} on R in equation (4) can be used to constrain the variation of number density n with size r within a core. For a spherical cloud with $\Delta v_{\text{NT}} = b_{\text{NT}} r^{p_{\text{NT}}}$, the density can be written

$$n = \frac{3}{4\pi m G r^2} \left(\frac{\mathcal{G}}{2\mathcal{K}} \right) \left[\frac{kT}{m} + \left(\frac{1 + 2p_{\text{NT}}}{8 \ln 2} \right) (b_{\text{NT}} r^{p_{\text{NT}}})^2 \right] \quad (6)$$

where G is the gravitational constant, and \mathcal{K} and \mathcal{G} are, respectively, the kinetic and gravitational energy, assuming that $\mathcal{G}/2\mathcal{K}$ is independent of r . At each r we assume $T = 10$ K and the core is in virial equilibrium (neglecting any surface pressure) so that $2\mathcal{K} = \mathcal{G}$, giving

$$n = 34(r/\text{pc})^{-2} + 1054(r/\text{pc})^{-0.6} \text{ cm}^{-3}. \quad (7)$$

This density is the sum of a “thermal” component where

$n \propto r^{-2}$ and “nonthermal” component where $n \propto r^{-0.6}$. The two components are equal at $r_0 = 0.09$ pc, which divides the primarily thermal core interior from the primarily nonthermal core exterior.

We note that the “thermal” density component may be “smoother” than the “nonthermal” density component in its degree of small-scale density fluctuations. The coupling of the nonthermal core gas is probably better than that of the thermal core gas to the large volume of lower density gas around the nonthermal core, and thus to disturbances arising from the differential illumination and heating, winds from neighboring stars, and magnetic waves. Furthermore, primarily thermal gas should disperse fluctuations of all sizes at the sound speed. The response to fluctuations by primarily nonthermal gas is less certain, because of our poor knowledge of its magnetic and turbulent structure. If the nonthermal gas is clumpier than the thermal gas, the clumpy core structure deduced from analysis of nonthermal lines such as CS (e.g., Mundy et al. 1986) may be consistent with the analysis of NH_3 , $C^{18}O$, and CS emission presented here.

If the density distribution is modeled as a single power law with radius, $n \propto r^{-q}$, then the density can be expressed as

$$n = \frac{3}{4\pi m G r^2} \left(\frac{\mathcal{G}}{2\mathcal{K}} \right) \left[\frac{1 + 2p_{\text{TOT}}}{8 \ln 2} (b_{\text{TOT}} r^{p_{\text{TOT}}})^2 \right], \quad (8)$$

where $\Delta v_{\text{TOT}} = b_{\text{TOT}} r^{p_{\text{TOT}}}$. Assuming virial equilibrium and the values in equation (4) gives

$$n = 194(r/\text{pc})^{-1.6} \text{ cm}^{-3}. \quad (9)$$

Determinations of the density structure in the outer regions of cores from line width size analyses (Snell 1981) and extinction measurements (Stüwe 1990; Cernicharo, Bachiller, & Duvert 1985) indicate $q = 1 \rightarrow 1.3$, a shallower slope than found here for the inner regions. This difference suggests that the inner regions of the cores sampled by the observations presented here have a steeper density profile than the outer regions. A similar steepening of the density profile in the inner regions of cores is suggested by recent submillimeter observations of the young, embedded stars (Ladd et al. 1991). Such a change of slope in the density profile might be expected when the core material makes the transition from nonthermal to thermal support. On the other hand, some determinations of the density profile based on molecular line column densities suggest that the envelopes of cores have profiles as steep as those deduced here for the inner core material (Snell 1981; Martin & Barrett 1978). However, determinations of the density profiles, especially from single molecular lines, are uncertain because of uncertainties in the molecular abundance and the excitation temperature. Further work is clearly needed in this area.

If $\mathcal{G}/2\mathcal{K}$ is independent of r , equation (8) shows that if the density can be described as a power law in size, then the line width must also be a power law in size. For example, if $\mathcal{G}/2\mathcal{K}$ has only a small variation over the range of r considered, then a small range of column density implies $\Delta v_{\text{TOT}} \propto r^{0.5}$, as seen in some studies (e.g., Snell 1981). On the other hand, if $\mathcal{G}/2\mathcal{K}$ varies sufficiently from cloud to cloud, such as could occur for unbound clouds, there would not be a simple correlation between line width and size. Such a cloud-to-cloud variation might account for the poor correlation of line width with size seen in some recent studies of molecular clouds (Lada, Bally, & Stark 1991; Loren 1989).

4.3. Implications of $\Delta v_{\text{NT}}(R)$

The variation of the nonthermal part of the line width with radius (eq. [5]) combined with the density profile within a core (eq. [9]) shows that the nonthermal pressure varies as $\propto r^{-0.2}$. If the nonthermal pressure is magnetic (Myers & Goodman 1988) this implies that the magnetic field should vary as $r^{-s/2}$ with $s/2 = 0.15 \rightarrow 0.05$. In other words, if the nonthermal component of the line width reflects support by a magnetic field within the cores, the magnetic field strength does not vary significantly over the range of sizes, ~ 0.02 – 0.25 pc, sampled by the observations discussed in this paper. In terms of the core density, the magnetic field varies as $n^{0.05}$. This very weak dependence of the magnetic field on density is not necessarily evidence for ambipolar diffusion in these regions even though models of core formation which include ambipolar diffusion such as those of Lizano & Shu (1989) find a relatively uniform magnetic field as a function of density within the core. Tomisaka, Ikeuchi, & Nakamura (1988) have shown that for flux frozen clouds with relatively low degrees of central condensation and a significant thermal support, the magnetic field can have a very weak dependence on density. The much steeper variation of magnetic field with density which is usually associated with flux freezing is only evident in very condensed or else magnetically dominated regions (Tomisaka et al. 1988).

In comparison to larger size scales in clouds where $\Delta v_{\text{NT}} \sim \Delta v_{\text{TOT}} \sim R^{0.5}$ (e.g., Snell 1981), the nonthermal component of line width decreases much more rapidly toward the interiors of the small cores discussed here where $\Delta v_{\text{NT}} \sim R^{0.7}$ (eq. [5]). This suggests that the nonthermal motions are more efficiently damped at the small size scales of dense cores. If the nonthermal motions in clouds are due to Alfvén waves, then there is a characteristic minimum wavelength below which the waves are strongly damped and can no longer propagate (Mouschovias & Morton 1991). The steepening of $\Delta v_{\text{NT}}(R)$ in the inner regions of these cores may indicate such an effect.

5. CONCLUSIONS

The results presented here are based on molecular line spectra and maps of 14 dense cores, each observed in three lines of CS, C¹⁸O, and NH₃. Our main conclusions are as follows:

1. For all three lines, the velocity FWHM of a line and the spatial FWHM of the line intensity are significantly correlated, with $\Delta v_{\text{obs}} \propto R^{p_{\text{obs}}}$, with $p_{\text{obs}} = 0.4 \pm 0.1$, for eight cores with an associated star of typical luminosity $2 L_{\odot}$, and also for six starless cores. This “line width–size” relation, and the physical conditions it represents, are thus largely independent of the presence or absence of an associated star.

2. The line width–size relation for starless cores has essentially the same intercept and the same slope from line to line for a typical core, as it has over all lines and cores. Therefore these relations reflect *internal* core structure and motions which vary relatively slightly from core to core and do not reflect large variations in structure and motions from core to core.

3. The correlation of *observed* line width and size implies two other useful relations. The velocity FWHM Δv_{TOT} of the molecule of mean mass varies with map size R as a power law, with $p_{\text{TOT}} = 0.20 \pm 0.04$. The velocity FWHM of the nonthermal component of the motions Δv_{NT} varies as a power law, with $p_{\text{NT}} = 0.7 \pm 0.1$.

4. Since the cores are in virial equilibrium, the variation of Δv_{TOT} with size implies that the density, n , within a core can be approximated as a single power, $n = 194(r/\text{pc})^{-1.6} \text{ cm}^{-3}$. For an isothermal core, whose nonthermal motions scale with radius as $r^{p_{\text{NT}}}$ the density profile can be written as a “thermal” component with $n \propto r^{-2}$ and a nonthermal component with $n \propto r^{-2+2p_{\text{NT}}}$. Assuming a core temperature of 10 K, the data in this paper imply that these two components are equal at $r_0 = 0.09$ pc, which is the radius which divides the primarily thermal core interior from the primarily nonthermal core exterior.

5. A core in virial equilibrium, with line width–size relation typical of the sample in this paper, has nonthermal pressure which varies with radius as $r^{-0.2}$ and with density as $n^{0.1}$. If the nonthermal pressure is largely magnetic, the corresponding field strength varies with density as $n^{0.05}$.

G. A. F. acknowledges the support of NSF grant AST87-14721 to the Radio Astronomy Laboratory, University of California, Berkeley, a Smithsonian Astrophysical Observatory Predoctoral Fellowship, and a Harvard-Smithsonian Center for Astrophysics Fellowship.

REFERENCES

- Benson, P. J., & Myers, P. C. 1989, *ApJS*, 71, 89 (BM)
 Cernicharo, J., Bachiller, R., & Durtver, G. 1985, *A&A*, 149, 273
 Chieze, J. P. 1987, *ApJ*, 171, 225
 Dame, T. M., Elmegreen, B. G., Cohen, R. S., & Thaddeus, P. 1986, *ApJ*, 305, 892
 Elmegreen, B. G. 1989, *ApJ*, 338, 178
 Falgarone, E., & Perault, M. 1987, in *Physical Processes in Interstellar Clouds*, ed. G. E. Morfill & M. Scholer (Dordrecht: Reidel), 59
 Fleck, R. C. 1983, *ApJ*, 272, L45
 ———. 1988, *ApJ*, 328, 299
 Fuller, G. A. 1989, Ph.D. thesis, Univ. of California, Berkeley
 Goldsmith, P. F., Langer, W. D., & Wilson, R. W. 1986, *ApJ*, 303, L11
 Heyer, M. H., Snell, R. L., Goldsmith, P. F., & Myers, P. C. 1987, *ApJ*, 321, 370
 Kegel, W. H. 1989, *A&A*, 225, 517
 Lada, E. A., Bally, J., & Stark, A. A. 1991, *ApJ*, 368, 432
 Ladd, E. F., Adams, F. C., Casey, S., Davidson, J. A., Fuller, G. A., Harper, D. A., Myers, P. C., & Padman, R. 1991, *ApJ*, 366, 203
 Larson, R. B. 1981, *MNRAS*, 194, 809
 Leung, C. M., Kutner, M. L., & Mead, K. N. 1982, *ApJ*, 262, 583
 Lizano, S., & Shu, F. H. 1989, *ApJ*, 342, 834
 Loren, R. B. 1989, *ApJ*, 338, 925
 Martin, R. N., & Barrett, A. H. 1978, *ApJS*, 36, 1
 McKee, C. F. 1989, *ApJ*, 345, 782
 Mouschovias, T. Ch., & Morton, S. A. 1991, *ApJ*, 371, 296
 Mundy, L. G., Snell, R. L., Evans, N. J., Goldsmith, P. F., & Bally, J. 1986, *ApJ*, 306, 670
 Myers, P. C. 1983, *ApJ*, 270, 105
 Myers, P. C., Fuller, G. A., Goodman, A. A., & Benson, P. J. 1991a, *ApJ*, 376, 561
 Myers, P. C., Fuller, G. A., Mathieu, R. D., Beichman, C. A., Benson, P. J., Schild, R. E., & Emerson, J. P. 1987, *ApJ*, 319, 340
 Myers, P. C., & Goodman, A. A. 1988, *ApJ*, 329, 392
 Myers, P. C., Heyer, M. H., Snell, R. L., & Goldsmith, P. F. 1988, *ApJ*, 324, 907
 Myers, P. C., Ho, P. T. P., Schneps, M. H., Chin, G., Pankonin, V., & Winnberg, A. 1978, *ApJ*, 220, 864
 Myers, P. C., Ladd, E. F., & Fuller, G. A. 1991b, *ApJ*, 372, L95 (MLF)
 Parker, N. D., Padman, R., Scott, P. F., & Hills, R. E. 1988, *MNRAS*, 234, 67P
 Phillips, T. G., Huggins, P. J., Wannier, P. G., & Scoville, N. Z. 1979, *ApJ*, 231, 720
 Scoville, N. Z., Sanders, D. B., & Clemens, D. P. 1986, *ApJ*, 310, L77
 Snell, R. L. 1981, *ApJS*, 45, 121
 Solomon, P. M., Rivolo, A. R., Barrett, J., & Yahil, A. 1987, *ApJ*, 319, 730
 Stüwe, J. A. 1990, *A&A*, 237, 178
 Tomisaka, K., Ikeuchi, S., & Nakamura, T. 1988, *ApJ*, 335, 239
 Torrelles, J. M., Rodriguez, L. F., Cantó, J., Carral, P., Marcaide, J., Moran, J. M., & Ho, P. T. P. 1983, *ApJ*, 274, 214
 Ungerechts, H., Walmsley, C. M., & Winnewisser, G. 1982, *A&A*, 111, 339
 Zhou, S., Wu, Y., Evans, N. J., Fuller, G. A., & Myers, P. C. 1989, *ApJ*, 346, 168